



Adsorption and removal of arsenite on ordered mesoporous Fe-modified ZrO₂

Xiaofei Sun, Chun Hu*, Jiuhui Qu

State Key Laboratory of Environmental Aquatic Chemistry, Research Center for Eco-Environmental Sciences, Chinese Academy of Sciences, Beijing 100085, China

Tel. +86 10 6284 9628; Fax +86 10 6292 3541; email: huchun@rcees.ac.cn

Received 10 October 2008; accepted 14 June 2009

ABSTRACT

A new adsorbent, ordered mesoporous Fe-modified ZrO₂, was prepared and applied for the adsorption of arsenite [As(III)] and arsenate [As(V)] from water. The adsorbent showed higher efficiency for the removal of As(III) and As(V) than that of unmodified mesoporous ZrO₂, especially of As(III) without pre-oxidation. The maximum uptake at pH 7.0 was 80 mg g⁻¹ for As(III) and 45 mg g⁻¹ for As(V). The behavior of arsenic adsorption onto Fe-modified ZrO₂ was investigated by adsorption isotherms, adsorption kinetics, and the effect of pH on adsorption. The adsorption equilibrium of arsenite was rapid, with 90% adsorption within 1 h. Furthermore, the interactions of As(V) and As(III) with adsorbent were investigated using electrophoretic mobility (EM) measurements and Fourier transform infrared (FTIR) spectroscopy. The adsorption of As(V) and As(III) decreased the isoelectric point of Fe-modified ZrO₂ from 6.00 to 3.00 and 4.51, respectively, suggesting the formation of negatively charged inner-sphere complexes for both arsenic species. The results of FTIR suggested that the –OH band on the surface was the adsorption sites. The more adsorption sites were formed on mesoporous ZrO₂ modified with Fe, which possessed abundant surface hydroxyl groups, resulting higher efficiency for arsenic removal.

Keywords: Mesoporous zirconia; Fe-modified; Adsorption; Arsenic; Mechanism

1. Introduction

Arsenic is a ubiquitous element that ranks 20th in abundance in the earth's crust. It is a carcinogen and is toxic to humans and other organisms [1]. The global cycling of arsenic is expected to increase due to the progressive industrialization of developing nations, which will pose potentially serious environmental problems throughout the world. The chronic toxicity of arsenic in drinking water is known to cause blackfoot disease and various types of cancer [2]. Therefore, removal of arsenic is one of the most important water treatment issues.

The most common valence states of arsenic in water are the oxidized (+V oxidation state, arsenate, As(V)) and reduced (+III oxidation state, arsenite, As(III)) forms. As(III) is more mobile and more toxic (25–60 times) than As(V) [3]. Removal of As(III) from aqueous solutions is usually poor compared to that of As(V) by almost all of the technologies evaluated. This is because the predominant As(III) compound has a neutral charge, while the As(V) species are negatively charged in pH > 2. In general, the achievement of enhanced As(III) removal can be achieved by converting As(III)–As(V) through pre-oxidation [4]. The prior oxidation of the trivalent form of arsenic into the less toxic pentavalent form is an important stage in the treatment since arsenate (AsO₄³⁻, As(V)) is removed more

*Corresponding author

effectively than arsenite (AsO_3^{3-} , As(III)) [5,6]. But this method is too costly in terms of investment and running costs to be applied in plants of low flows ($<10 \text{ m}^3/\text{h}$) in sparsely inhabited zones [7]. Therefore, it is essential that methods that allow those installations to supply drinkable water at low cost should be developed.

Adsorption is considered to be less expensive than membrane filtration, easier and safer to handle compared to the contaminated sludge produced by the precipitation method, and more versatile than the ion exchange technique [4,8]. The uptake and kinetics of arsenic have been investigated for metal-loaded activated carbon [9], coral limestone [10], ferric (hydr)oxides [11], active alumina [12], mesoporous alumina [13], and other substances. However, removal of As(III) from aqueous solutions by most of these substances is usually poor compared to that of As(V) without pre-oxidation.

Nanoporous materials offer many advantages, making them good candidates as adsorbents to remove arsenic from water due to their exceptionally high surface area, open porosity, and ease of chemical modification. For example, mesoporous alumina has shown higher adsorption capacity than activated alumina [13]. However, the maximum uptake of As(III) was lower than that of As(V). Recently, surface functionalization of ordered mesoporous material has garnered intense interest for use. Puanngam and Unob [14] found that the chemically modified MCM-41 had better ability for Hg(II) ion adsorption than modified silica gel. Unob et al. [15] used the iron oxide modified waste silica to obtain an effective adsorbent for metal removal from wastewater. Yusof and Malek [16] found that the HDTMA-modified zeolite Y had better adsorption capacities of Cr(VI) and As(V) than that of unmodified zeolite Y. These mean that the structure of the materials affects the adsorption behavior.

We have synthesized ordered mesoporous Fe-modified ZrO_2 by a novel solid-state reaction method [17]. The order mesoporous Fe-modified ZrO_2 had better adsorption capacities of As(III) and As(V) than that of order mesoporous ZrO_2 . In the present study, for the first time, the mechanism and kinetics of the adsorption and removal of As(III) using this new ordered mesoporous Fe-modified ZrO_2 were researched. The adsorbent was found to be effective for the removal of As(III) at neutral condition, and the adsorption capacity was $80 \text{ mg}_{\text{As(III)}} \text{ g}^{-1}$ and $45 \text{ mg}_{\text{As(V)}} \text{ g}^{-1}$, respectively. Furthermore, the adsorption behavior of As(III) on Fe-modified ZrO_2 was elucidated by electrophoretic mobility (EM) measurements as well as Fourier transform infrared (FTIR) spectroscopy.

2. Experimental

2.1. Sample preparation

Mesoporous nanosize Fe-modified ZrO_2 was prepared via solid-state reaction using the structure-directing method [17]. In this synthesis, 12 g of $\text{ZrOCl}_2 \cdot 8\text{H}_2\text{O}$, 0.4 g $\text{FeCl}_3 \cdot 6\text{H}_2\text{O}$, and 8 g block-copolymer surfactant $\text{HO}(\text{CH}_2\text{CH}_2\text{O})_x(\text{CH}_2\text{CH}(\text{CH}_3)\text{O})_y(\text{CH}_2\text{CH}_2\text{O})_x\text{H}$ (fw = 5800) were milled together in a mortar and then reacted with 6 g of milled NaOH under vigorous stirring. The resulting product was transferred to an autoclave to crystallize. The crystallizing time and temperature were 48 h and 383 K. After crystallization, the product was washed with deionized water until it was free of Cl^- ions and then washed with ethanol twice to remove water. Finally, the sample was dried at 383 K overnight and calcined at 623 K for 3 h. The mesoporous ZrO_2 was synthesized by the same method without the addition of $\text{FeCl}_3 \cdot 6\text{H}_2\text{O}$.

2.2. Characterization

Powder X-ray diffraction (XRD) was recorded on a Scintag-XDS-2000 diffractometer with Cu $K\alpha$ radiation ($\lambda = 1.54059$). Nitrogen adsorption/desorption experiments of Fe-modified ZrO_2 and mesoporous ZrO_2 were carried out using a Micromeritics ASAP2000 analyzer (Micromeritics Co., USA). FTIR spectra of Fe-modified ZrO_2 , mesoporous ZrO_2 , and general ZrO_2 before and after adsorption were recorded on a FTIR spectrometer (Nicolet 5700).

2.3. Batch adsorption tests

Adsorption isotherms were conducted by batch experiments at 20°C , pH 7.0 [18]. The experiments were carried out in 150 mL stoppered conical flasks containing 100 mL of arsenic [sodium arsenate ($\text{Na}_3\text{AsO}_4 \cdot 12\text{H}_2\text{O}$; AR) or sodium arsenite (NaAsO_2 ; AR)] solutions with concentrations: $1\text{--}35 \text{ mg L}^{-1}$, with adsorbent: 0.1 g L^{-1} . To analyze the effects of pH, the equilibrium adsorption of arsenite and arsenate was measured at different pH levels from 3 to 10 by setting the initial arsenic concentration at 5 mg L^{-1} with adsorbent: 0.1 g L^{-1} . The initial pH of the solution was adjusted by 0.1 M HCl and NaOH solutions. The flasks were shaken at 180 rpm in a shaker for 24 h and then the suspension was passed through a membrane filter ($0.45 \mu\text{m}$) for analysis. Arsenic was analyzed on an atomic fluorescence spectrometer (HG-AFS-610, Beijing Rayleigh Analytic Instrument Corporation, China). Experiments were repeated three times, and all of the data

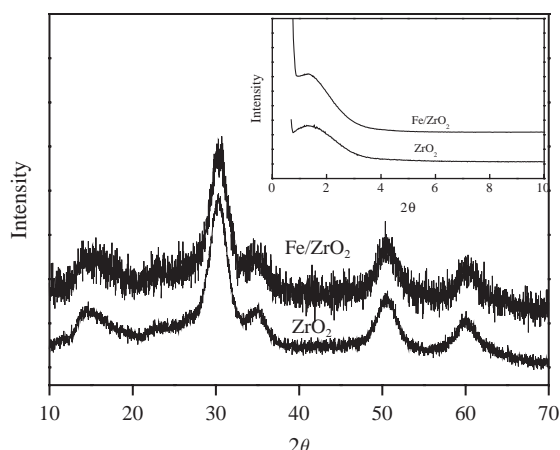


Fig. 1. XRD pattern of mesoporous ZrO_2 and Fe-modified ZrO_2 . The inset shows the low-angle peak.

are the average of the three. Kinetic study was consulted reference [13]. Kinetic studies were carried out for different time periods, using buffer solution pH 6, in 15-min intervals (5, 15, 30, 45, 60...120 min), according to the above procedure for different concentrations. The initial arsenic concentration was 10 mg L^{-1} , the adsorbent was 1 g L^{-1} , and the initial pH was 7.0.

2.4. EM measurement

The EM was determined using a Zetasizer 2000 (Malvern Co., UK). Suspensions contain 0.1 g L^{-1} Fe-modified ZrO_2 in KNO_3 (10^{-3} M) solutions with or without 50 mg L^{-1} arsenic were placed in a shaker and shaken for 24 h as reference [19]. The pH was adjusted to between 1 and 11 using dilute NaOH and HCl solutions. Every reading of the instrument was recorded after three consistent readings had been attained and averaged.

3. Results and discussion

3.1. Characterization of the adsorbents

Fig. 1 shows the XRD patterns of Fe-modified ZrO_2 and mesoporous ZrO_2 . As can be noted from this figure depicted in the inset of Fig. 1, the low angle XRD patterns of all products gave a clear diffraction peak, even though not sharp, located at around 2° , which can be assigned to the ordered mesostructure [20]. In the wide-angle region of the XRD patterns (Fig. 1), the two samples exhibits diffraction peaks at ca. 30° , 35° , 50° , and 60° , assigned to tetragonal phase of crystalline ZrO_2 [20,21]. This indicates that the functionalization of mesoporous ZrO_2 did not lead to a structural change. The same phenomenon was observed by Puanngam and Unob [14]. Nitrogen adsorption/

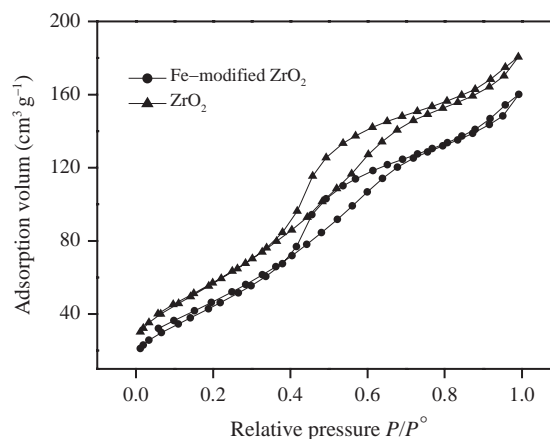


Fig. 2. N_2 adsorption/desorption isotherm for mesoporous ZrO_2 and Fe-modified ZrO_2 .

desorption isotherms of mesoporous ZrO_2 and Fe-modified ZrO_2 were typically the IV type with large hysteresis loops, indicating the presence of a mesoporous structure [17], shown in Fig. 2. Moreover, an H4 hysteresis loop was observed, implying that the samples have intraparticle and ordered porosity [22]. The specific surface areas of the Fe-modified ZrO_2 and ZrO_2 were 229 and $231 \text{ m}^2 \text{ g}^{-1}$, respectively. The modification leads to a little reduction in surface area. This is probably due to the occupation of the functionalized molecules on the surface and inside the pores of the adsorbent [14,15]. The Fe amount was a little, so the reduction of the surface area was not great. As a reference, the general ZrO_2 was also characterized by nitrogen adsorption/desorption isotherms. The results indicated that the general ZrO_2 was nonporous, and the specific surface area was $8.83 \text{ m}^2 \text{ g}^{-1}$.

3.2. Adsorption isotherms

To compare the adsorption capacities of Fe-modified ZrO_2 , mesoporous ZrO_2 and general ZrO_2 , series adsorption isotherms were investigated. Fig. 3 presents the experimental adsorption isotherms for arsenic removal when the initial concentrations of arsenic were in the range of $1\text{--}35 \text{ mg L}^{-1}$ at 20°C and pH 7.0. It was found that, Fe-modified ZrO_2 had the highest adsorption capacity, the adsorption capacity was $80 \text{ mg}_{As(III)} \text{ g}^{-1}$ and $45 \text{ mg}_{As(V)} \text{ g}^{-1}$, respectively. The adsorption capacity of arsenite was higher than mesoporous alumina [13]. The adsorption capacity for arsenite and arsenate by mesoporous ZrO_2 was $45 \text{ mg}_{As(III)} \text{ g}^{-1}$ and $18 \text{ mg}_{As(V)} \text{ g}^{-1}$, respectively. While, for the general ZrO_2 there was no adsorption capacity for arsenic. Obviously, through modification could increase the adsorption capacity of arsenic.

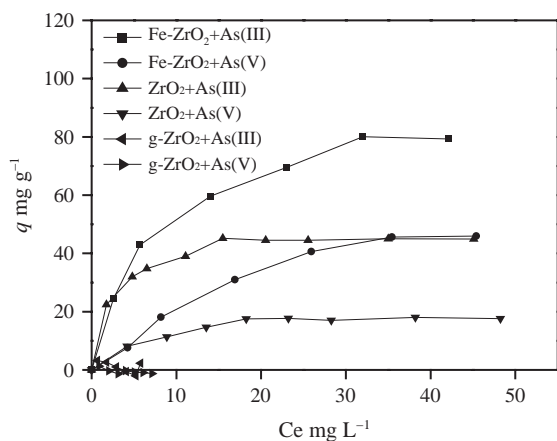


Fig. 3. Adsorption isotherms for arsenite and arsenate by Fe-modified ZrO_2 , mesoporous ZrO_2 and general ZrO_2 (adsorbent, 0.1 g L^{-1} ; arsenic concentration, $1\text{--}35 \text{ mg L}^{-1}$ at 20°C , $\text{pH } 7.0$).

3.3. FTIR spectroscopy

According to the surface complex model theory [23], metal hydroxyl groups ($M\text{--OH}$) on the surface of many metal oxides, which can be detected by IR spectroscopy, are the most abundant and reactive adsorption sites for anions. To reveal why these samples had different adsorption capacities, FTIR spectra was investigated. Therefore, the FTIR spectra of the --OH region for Fe-modified ZrO_2 , mesoporous ZrO_2 , and general ZrO_2 before and after adsorbing As(V) and As(III) were characterized. To ensure quantitative $Zr\text{--OH}$ analysis, the samples were mixed with KBr at a fixed ratio (1%). The same amount of fixed powder was also used to prepare the pellets for FTIR. The FTIR spectra of Fe-modified ZrO_2 after adsorbing As(V) or As(III) clearly indicated that the OH bands at 1048,

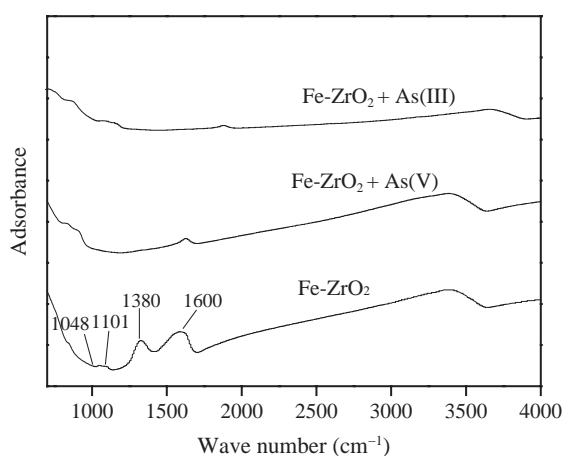


Fig. 4. FTIR spectra of Fe-modified ZrO_2 before and after adsorption of arsenic.

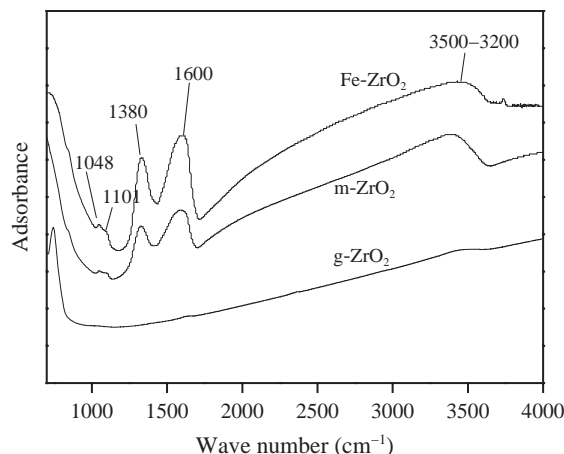


Fig. 5. FTIR spectra of Fe-modified ZrO_2 , mesoporous ZrO_2 and general ZrO_2 .

1101, and 1380 cm^{-1} gradually disappeared, and the peak at 1600 cm^{-1} became smaller after arsenic was adsorbed (Fig. 4), indicating that the replacement of --OH_2 or --OH occurred with the adsorption of arsenic. Fig. 5 presents variations of FTIR spectra for the Fe-modified ZrO_2 , mesoporous ZrO_2 and general ZrO_2 . The FTIR spectra of Fe-modified ZrO_2 had three kinds of --OH bands. The first type included $3500\text{--}3200 \text{ cm}^{-1}$, corresponding to the stretching of --OH groups of adsorbed water, which formed hydrogen bonds [24], and 1600 cm^{-1} , assigned to the bending vibration of adsorbed water [24]. The second type, 1380 cm^{-1} , could be attributed to the deformation vibration of $Zr\text{--OH}$ [25]. The last type was 1101 and 1048 cm^{-1} , assigned to the bending vibration of $Zr\text{--OH}$ [26]. Mesoporous ZrO_2 had the same variations with Fe-modified ZrO_2 basically. But the modified with Fe the peak at 1101, 1048, 1380, and 1600 cm^{-1} was stronger than mesoporous ZrO_2 . In contrast, there was no --OH groups on the general ZrO_2 , except bands corresponding to weak --OH stretching vibration (3400 cm^{-1}). It is quite possible that more --OH groups on the surface of the adsorbent led to a higher capacity to adsorb As(V) and As(III) . Mesoporous ZrO_2 modified with Fe enhanced the --OH groups on the surface, so the adsorption capacity increased.

3.4. Effect of pH on arsenic adsorption

To determine the optimum pH for the adsorption of arsenic on Fe-modified ZrO_2 , the adsorption of arsenic as a function of pH was studied. In general, the removal rate of As(V) decreased with increasing pH. Also, the adsorption of As(V) was reduced from 36 to 0 mg g^{-1} onto Fe-modified ZrO_2 as the pH shifted from 3 to 10, as shown in Fig. 6. In a wide range of pH (3–10),

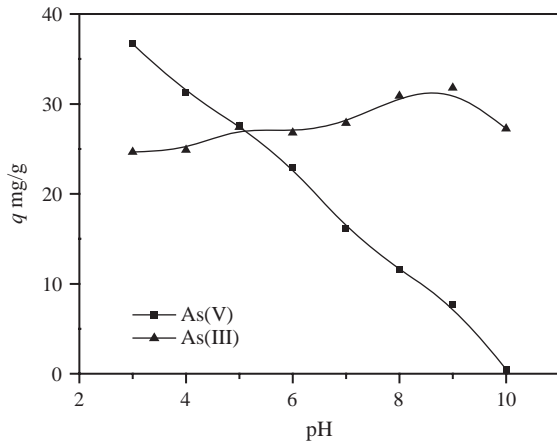
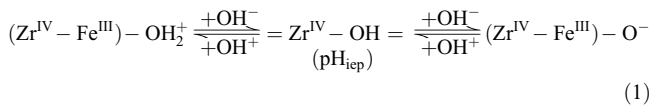


Fig. 6. Arsenic adsorption onto Fe-modified ZrO₂ at various initial pH values (adsorbent, 0.1 g L⁻¹; initial arsenic concentration, 5 mg L⁻¹).

the amount of As(III) adsorbed steadily approached about 30 mg g⁻¹, and the maximum uptake for As(III) 31.7 mg g⁻¹ was obtained at an initial pH of 9. The surface charge of the adsorbent and the speciation of arsenic in solution were significantly affected by pH. The isoelectric point of Fe-modified ZrO₂ (pH_{iep}) was about 6.0. At pH < 6.0, the surface of the adsorbent was positively charged, while it was negatively charged at pH > 6.0, as presented in Eq. (1):



The arsenate species and the corresponding pH values for their stability were H₃AsO₄ (pH < 2), H₂AsO₄⁻ (pH 2–7), HAsO₄²⁻ (pH 7–11), and AsO₄³⁻ (pH > 12). Therefore, at pH < 6.0, electrostatic attraction existed between H₂AsO₄⁻ and the adsorbent, leading to greater adsorption of As(V). At pH > 6.0, the electrostatic repulsive force between HAsO₄²⁻ or AsO₄³⁻ and the adsorbent increased with the increase of pH due to the more negative zeta potential of the adsorbent. This led to the reduction of As(V) adsorption. Similarly, trivalent arsenic is stable as neutral H₃AsO₃ at pH < 9, while H₂AsO₃⁻, HAsO₃²⁻, and AsO₃³⁻ are stable species in the pH ranges of 9–12, 12–13, and >13, respectively. Since arsenite species have a lower negative charge compared to arsenate species in the pH range of 3–9, they do not exhibit as much repulsion, and as a result, arsenite was preferably adsorbed by Fe-modified ZrO₂ in a wide pH range. In the pH range of 4–9, the predominant species was H₃AsO₃. In this connection, arsenite can be adsorbed through specific adsorption between the neutral species and positively

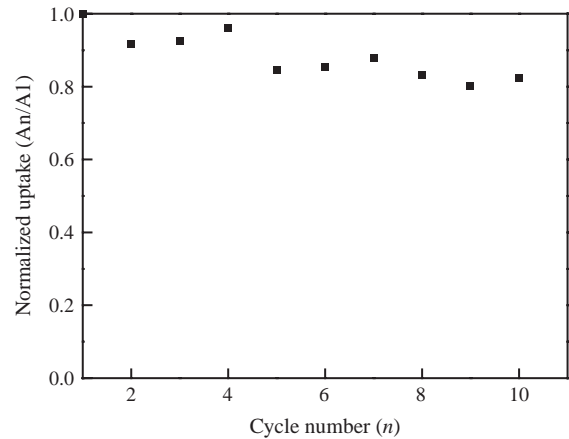


Fig. 7. Normalized adsorption change of Fe-modified ZrO₂ with the adsorption–desorption cyclic operation.

charged surface sites at lower pH values. The decrease in the adsorption yield at pH above 9 may be attributed to a higher negative charge of arsenite species and the negative charge of the adsorbent. The same results also were found by several other researchers [27,28]. The effect of pH on the adsorption correspond with the result of FTIR that OH or OH₂ was the adsorption sites. Arsenite was preferably adsorbed by Fe-modified ZrO₂ in a wide pH range. Although optimal arsenate removal was found in acidic conditions, high removal performance was still observed near neutral pH. In general, the pH of natural water is in the range of 6–8.5, so the pH does not need to be pre-adjusted for contaminated groundwater for the use of Fe-modified ZrO₂.

The experiments of the effects of pH verified that the adsorption of arsenic was low at high pH. Adsorbed arsenic ions can be desorbed from Fe-modified ZrO₂ by alkaline media. Therefore, desorption tests were carried out using 1 M sodium hydroxide solutions. Moreover, the feasibility of the adsorption–desorption cyclic operation was studied to investigate the long-term performance of Fe-modified ZrO₂. More than 80% of the initial adsorption capacity of Fe-modified ZrO₂ was maintained after 10 times of adsorption–desorption cycles (Fig. 7), where the adsorption capacity (A_n) of reused Fe-modified ZrO₂ was normalized with that of new Fe-modified ZrO₂ (A₁). The results showed that Fe-modified ZrO₂ could undergo repeated adsorption–desorption cycles without loss of activity.

3.5. Adsorption kinetics

The kinetics of adsorption, which describes the solution uptake rate governing the residence time of

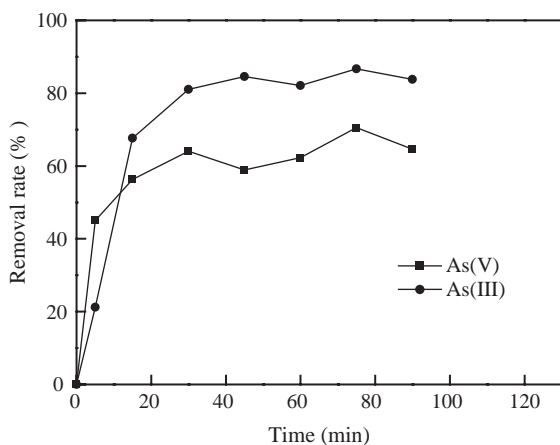


Fig. 8. Arsenic removal rate versus time by Fe-modified ZrO_2 (adsorbent, 0.2 g L^{-1} ; initial arsenic concentration, 10 mg L^{-1} , initial pH 6.0).

the adsorption reaction, is one of the important characteristics that define the adsorption efficiency. Hence, the kinetics of arsenic adsorption was analyzed to reveal the adsorption behavior of Fe-modified ZrO_2 . Fig. 8 shows the removal of arsenic by Fe-modified ZrO_2 at different times, and the simulations with the pseudo-second-order kinetic model and the intraparticle diffusion model are shown in Fig. 9A. The pseudo-second-order rate model is expressed as [29]:

$$t/q_t = 1/k_{ad}q_e^2 + t/q_e \quad (2)$$

where k_{ad} is the adsorption rate constant, q_t and q_e are the amount of metal ions adsorbed at time t and equilibrium, respectively. The initial adsorption rate h , as $t \rightarrow 0$ can be defined as:

$$h = k_{ad}q_e^2 \quad (3)$$

The intraparticle diffusion equation can be expressed as [29]:

$$q_t = k_{id}t^{1/2} \quad (4)$$

where k_{id} is the intraparticle diffusion rate constant, which can be determined by the slope of the straight-line portion of a plot of q_t versus $t^{1/2}$. The adsorption of As(III) and As(V) was rapid, occurring within 30 min, and promptly approached equilibrium. The removal rates of As(III) and As(V) were 90% and 80%, after 45 min, as shown in Fig. 8. The plots of t/q_t versus t were found to be straight lines for all arsenic species, and the value of correlation coefficient R^2 was extremely high ($R^2 > 0.99$) (Fig. 9A). These results suggested the applicability of pseudo-second-order kinetics to the present systems. The h value of As(V)

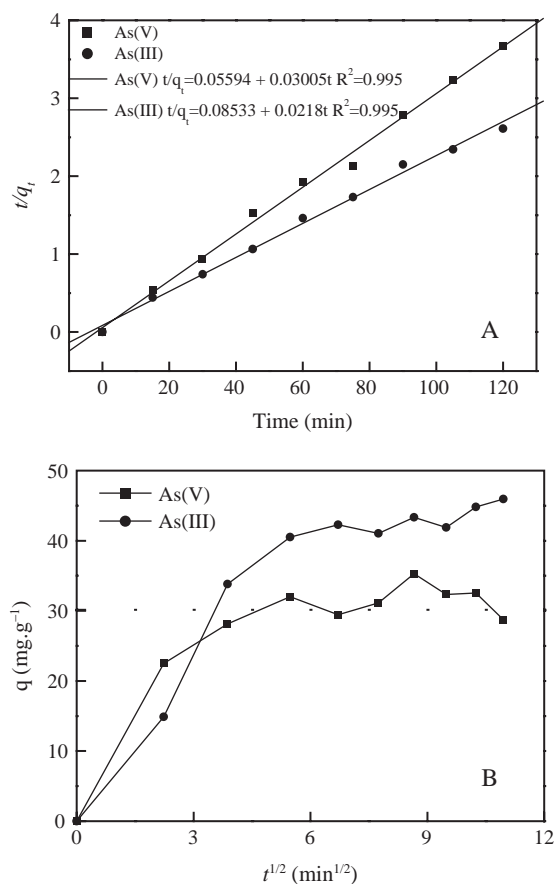


Fig. 9. (A) Pseudo-second-order adsorption rates of arsenite and arsenate adsorption to Fe-modified ZrO_2 . (B) Intraparticle diffusion rates of adsorption of arsenite and arsenate to Fe-modified ZrO_2 .

was higher than that of As(III) (17.88 and 11.7, respectively), meaning that As(V) was more easily adsorbed on Fe-modified ZrO_2 than As(III) at the initial adsorption stage. The plots of q_t against $t^{1/2}$ were multi-linear (Fig. 9B.), indicating that two steps occurred in the adsorption process. The first, sharper stage was the external surface adsorption and intraparticle diffusion stage, and the intraparticle diffusion was rate-controlled. When the adsorption at the exterior surface reached the saturation level, the arsenic ions began to enter the Fe-modified ZrO_2 via the pores within the particles and were adsorbed by the interior surfaces of the particles. When the arsenic ions were diffused into the pores of the Fe-modified ZrO_2 , the diffusion resistance increased, leading to a decrease in the diffusion rate. Subsequently, the intraparticle diffusion started to slow down due to the extremely low solute concentration in the solution and the diffusion resistance increased at the final equilibrium stage. In the system, the diffusion rate for As(V) (k_{id} , 12.5) was two

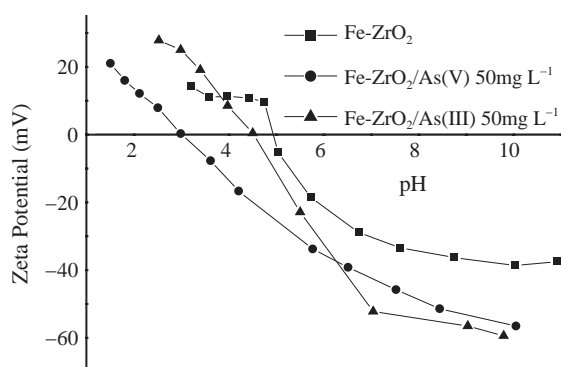


Fig. 10. Zeta potential for different suspensions of Fe-modified ZrO_2 (adsorbent, 0.1 g L^{-1} in the presence and absence of arsenic 50 mg L^{-1} with KNO_3 (10^{-3} M)).

times faster than that of As(III) (k_{id} , 5.9). This phenomenon indicated that arsenate ions are more easily diffused and transported into Fe-modified ZrO_2 than arsenite. The radius of an arsenate ion is smaller than that of an arsenite ion: HAsO_4^{2-} 3.97 Å, H_2AsO_4^- 4.16 Å, H_3AsO_3 4.16 Å, H_2AsO_3^- 4.80 Å, and H_3AsO_3 4.80 Å [8], which also suggests that arsenate ions are able to diffuse onto the pore channels of Fe-modified ZrO_2 more easily than arsenite ions.

3.6. EM

Fig. 10 shows the zeta potential of Fe-modified ZrO_2 in both the presence and absence of As(V) or As(III). The isoelectric point of Fe-modified ZrO_2 was about 5.00. It shifted to 4.51 after As(III) was adsorbed at an initial concentration of 50 mg L^{-1} , and shifted to 3.00 after As(V) was adsorbed at an initial concentration of 50 mg L^{-1} . The isoelectric point of metal oxide is determined by the protonation and deprotonation of surface hydroxyl groups. The formation of outer-sphere surface complexes cannot shift the isoelectric point because there are no specific chemical reactions between the adsorbate and the surface that could change the surface charge [19]. The shift of the isoelectric point to a lower pH range is evidence of the formation of anionic negatively charged surface complexes [30]. Therefore, the results implied that both As(V) and As(III) formed negatively charged inner-sphere complexes on Fe-modified ZrO_2 , which was verified by FTIR analysis.

4. Conclusion

A new adsorbent, ordered mesoporous Fe-modified ZrO_2 was prepared and applied for the adsorption of arsenite [As(III)] and arsenate [As(V)] from water. The

maximum uptake at pH 7.0 was $80 \text{ mg}_{\text{As(III)}} \text{ g}^{-1}$ for As(III) and $45 \text{ mg}_{\text{As(V)}} \text{ g}^{-1}$ for As(V). The adsorption equilibrium of arsenite was rapid, with 90% adsorption within 1 h. The results of FTIR suggested that the OH band on the surface was the adsorption sites. The more adsorption sites were formed on mesoporous ZrO_2 modified with Fe resulting higher efficiency for As(III) removal.

Reference

- [1] B.K. Mandal and K.T. Suzuki, *Talanta*, 58 (2002) 201-235.
- [2] V. Lenoble, O. Bouras, V. Deluchat, B. Serpaud and J.-C. Bollinger, *J. Colloid Interface Sci.*, 255 (2002) 52-58.
- [3] M.E. Pena, G.P. Korfiatis, M. Patel, L. Lippincott and X. Meng, *Water Res.*, 39 (2005) 2327-2337.
- [4] Y.-h. Xu, T. Nakajima and A. Ohki, *J. Hazard. Mater.*, 92 (2002) 275-287.
- [5] M. Borho and P. Wilderer, *Water Sci. Technol.*, 34 (1996) 25-31.
- [6] X. Meng, S. Bang and G.P. Korfiatis, *Water Res.*, 34 (2000) 1255-1261.
- [7] S.J. Hug, L. Canonica, M. Wegelin, D. Gechter and U. von Gunten, *Environ. Sci. Technol.*, 35 (2001) 2114-2121.
- [8] T.-F. Lin and J.-K. Wu, *Water Res.*, 35 (2001) 2049-2057.
- [9] T. Budinova, N. Petrov, M. Razvigorova, J. Parra and P. Galiatsatou, *Ind. Eng. Chem. Res.*, 45 (2006) 1896-1901.
- [10] Akira Ohki, Kensuke Naka and Shigeru Maeda, *Appl. Organometal. Chem.*, 10 (1996) 6.
- [11] Y. Jia and G.P. Demopoulos, *Environ. Sci. Technol.*, 39 (2005) 9523-9527.
- [12] T.S. Singh and K.K. Pant, *Sep. Purif. Technol.*, 36 (2004) 139-147.
- [13] Y. Kim, C. Kim, I. Choi, S. Rengaraj and J. Yi, *Environ. Sci. Technol.*, 38 (2004) 924-931.
- [14] M. Puanngam and F. Unob, *J. Hazard. Mater.*, 154 (2008) 578-587.
- [15] F. Unob, B. Wongsiri, N. Phaeon, M. Puanngam and J. Shiowatana, *J. Hazard. Mater.*, 142 (2007) 455-462.
- [16] A.M. Yusof and N.A.N.N. Malek, *J. Hazard. Mater.*, 162 (2009) 1019-1024.
- [17] X.M. Liu, G.Q. Lu and Z.F. Yan, *J. Phys. Chem. B*, 108 (2004) 15523-15528.
- [18] G. Zhang, J. Qu, H. Liu, R. Liu and R. Wu, *Water Res.*, 41 (2007) 1921-1928.
- [19] M. Pena, X. Meng, G.P. Korfiatis and C. Jing, *Environ. Sci. Technol.*, 40 (2006) 1257-1262.
- [20] S.-Y. Chen, L.-Y. Jang and S. Cheng, *J. Phys. Chem. B*, 110 (2006) 11761-11771.
- [21] Y. Sun, L. Yuan, S. Ma, Y. Han, L. Zhao, W. Wang, C.-L. Chen and F.-S. Xiao, *Appl. Catal. A Gen.*, 268 (2004) 17-24.
- [22] J.L. Blin, R. Flamant and B.L. Su, *Int. J. Inorg. Mater.*, 3 (2001) 959-972.
- [23] T. Stumm, *Chemistry of the Solid-Water Interface*, John Wiley, New York, 1992.
- [24] Y. Okamoto, T. Kubota, Y. Ohto and S. Nasu, *J. Phys. Chem. B*, 104 (2000) 8462-8470.
- [25] Q.Z. Dong and X. Shao, *Ion Exchange Adsorp.*, 22 (2006) 363-368.
- [26] Y. Zhang, M. Yang, X.M. Dou, H. He and D.S. Wang, *Environ. Sci. Technol.*, 39 (2005) 7246-7253.
- [27] K.P. Raven, A. Jain and R.H. Loeppert, *Environ. Sci. Technol.*, 32 (1998) 344-349.
- [28] S. Maity, S. Chakravarty, S. Bhattacharjee and B.C. Roy, *Water Res.*, 39 (2005) 2579-2590.
- [29] X.P. Liao and B. Shi, *Environ. Sci. Technol.*, 39 (2005) 4628-4632.
- [30] S. Goldberg and C.T. Johnston, *J. Colloid Interface Sci.*, 234 (2001) 204-216.